Polish J. Chem., **75**, 785–793 (2001)

A Novel Tetranuclear Iron Complex $[Fe_4O_2(O_2CC_2H_5)_7(bipy)_2]PF_6 \cdot 2H_2O$ (bipy = 2,2′-Bipyridine): Synthesis, Crystal Structure and Magnetic Properties

by B. Yan[1,2] and Z.D. Chen[1,2*]

[1]*State Key Laboratory of Rare Earth Material Chemistry and Applications, College of Chemistry and Molecular Engineering, Peking University, Beijing, 100871, P. R.. China*
[2]*Peking University-The University of Hong Kong, Joint Laboratory of Rare Earth Material and Bioinorganic Chemistry, Beijing, 100871, P. R.. China*

(Received November 16th, 2000; revised manuscript December 28th, 2000)

A novel tetranuclear iron-oxo complex has been synthesized and characterized by X-ray single crystal structural analysis: $[Fe_4O_2(O_2CC_2H_5)_7(bipy)_2]PF_6 \cdot 2H_2O$ (bipy = 2,2′-bipyridine). The title complex crystallizes in the monoclinic system, space group *C*2/*c*, with lattice parameters a = 27.859(2) Å, b = 13.0629(10) Å, c = 17.2698(14) Å, β = 123.6080(10)°, V = 5234.3 (7) Å^3, Dc = 1.559 Mg/m^3, Z = 4, R_1 = 0.0493. The molecular structure shows that there are two types of coordination environment for Fe(III) atoms. One is formed by two N atoms and four O atoms, another by six O atoms, all in distorted octahedron, which forms a "butterfly" core structure. The corresponding variable temperature susceptibility measurement shows the antiferromagnetic interactions in the complex.

Key words: synthesis, crystal structure, magnetic properties, iron, 2,2′-bipyridine, propionic acid, tetranuclear iron complex

The biological role of polynuclear oxo-, hydroxo-, and alkoxo-bridged iron systems has become a subject of considerable interest in the last few years [1–3]. The active sites in some metalloproteins systems such as hemerythrin [4,5], methane monooxygenase [6,7] and ribonucleotide reductase [8,9] may contain diiron cores, where the iron site can transfer from Fe_2^{II} to Fe_2^{III}. It is very surprising that very similar structures can exhibit variety of functions in the proteins. Studies on the synthesis of these model complexes to model the iron proteins have been extensively carried out and suggested how important their role in biological systems. Lippard and co-workers [10,11] obtained a novel tetranuclear molecule $(Et_4N)[Fe_4O_2(O_2CR)_7(H_2B(pz)_2)_2]$, (R = Me, Ph), where $H_2B(pz)_2^-$ is the dihydrobis(1-pyrazolyl)borate anion. This molecule contains Fe(III) ions disposed in a "butterfly" $[Fe_4O_2]^{8+}$ core. Hendrickson and co-workers [12] reported the molecular spin frustration in the $[Fe_4O_2]^{8+}$ core: $[Fe_4O_2(O_2CR)_7(bipy)_2](ClO_4)$ (R = Me, Ph). They studied the crystal structure, spec-

* Corresponding author, fax: 86-10-62751016, tel.: 86-10-62751708, e-mail: zdchen@pku.edu.cn

troscopic characteristics and especially gave a detailed theoretical analysis of the magnetic properties.

We obtained here a novel tetranuclear iron complex $[Fe_4O_2(O_2CC_2H_5)_7(bipy)_2]PF_6{\cdot}2H_2O$ (bipy = 2,2′-bipyridine), which exhibits the "butterfly" core structure $[Fe_4O_2]^{8+}$. The crystal structure and magnetic properties are discussed.

EXPERIMENTAL

Preparation of $[Fe_4O_2(O_2CC_2H_5)_7(bipy)_2]PF_6{\cdot}2H_2O$: All materials were reagent grade and used without further purification. To a stirred solution of $FeCl_3{\cdot}6H_2O$ (0.72 g, 2.67 mmol) in C_2H_5OH (20 mL) was treated with solid $NaO_2CC_2H_5$ (0.544 g, 6.63 mmol) and bipy (0.223 g, 1.43 mmol). After stirring for 15 min, $NaPF_6$ (0.41 g, 3.35 mmol) was added to the brown reaction mixture, and the resulting green-brown slurry was stirred overnight at ambient temperature. Deep brown single crystals suitable for X-ray crystal structure determination were obtained by slow evaporation of the filtrate at room temperature over some weeks. Yield 21%. Anal. Calcd. for $C_{41}H_{55}F_6Fe_4N_4O_{18}P$ (%): C, 40.06; H, 4.48; N, 4.60; F, 9.28. Found: C, 39.07; H, 4.40; N, 4.45; F, 9.05.

X-ray crystallography: Diffraction experiment of a good block brown crystal with dimensions 0.20 × 0.20 × 0.20 mm was performed with graphite-monochromated Mo Kα radiation on an Enraf-Nonius CAD4 four-circle diffractometer. The detailed crystal structure data and structure refinement parameters for the complex are listed in Table 1 and supplementary material. Crystallographic data have been deposited with the Cambridge Crystallographic Data Center (deposition number CCDC 152197). The structure was solved by direct method. Intensity data were measured using the ω-2θ scan technique and 4441 intensity reflections with $I \geq 2\sigma(I)$ were used in the refinements. All non-hydrogen atoms were refined anisotropically by full-matrix least-squares methods, which is given in Table 2. The hydrogen atoms were added geometrically and not refined. All calculations were performed on a 586PC computer using SHELXS-97 and refined with SHELXL-97.

Table 1. Crystal data and structure refinement.

Compound	$[Fe_4O_2(O_2CC_2H_5)_7(bipy)_2]PF_6{\cdot}2H_2O$
Color/shape	Brown/block
Empirical formula	$C_{41}H_{55}F_6Fe_4N_4O_{18}P$
Formula weight	1260.26
Temperature	293(2) K
Crystal system	Monoclinic
Space group	C_2/c
Unit cell dimensions	a = 27.859(2) Å
	b = 13.0629(10) Å
	c = 17.2698(14) Å
	β = 123.6080(10)°
Volume	5234.3(7) Å^3
Z	4
Density (calculated)	1.559 Mg/m^3
Absorption coefficient	1.206 mm^{-1}
Wavelength	0.71073 Å
F(000)	2520
Crystal size	0.20 × 0.20 × 0.20 mm
θ range for data collection	1.76 to 25.03°

Table 1 (continuation)

Reflections collected	10250
Independent/observed refls.	4441 (R_{int} = 0.0253)
Absorption correction	Sadabs
Range of relat. Transm. Factors	0.91 and 0.64
Refinement method	Full-matrix least-squares on F^2
Goodness-of-fit on F^2	1.013
Final R indices [I > 2σ(*I*)]	R_1 = 0.0493, wR_2 = 0.1273
Largest diff. peak and hole	0.930 and –0.829 e A^{-3}

Physical measurement: Elemental analyses for C, H, N, F were performed on an Elementar Carb EL elemental analyzer. Infrared spectra were recorded with a Nicolet 7199B spectrophotometer in the 4000–400 cm^{-1}on KBr pellet. The thermogravimetric analysis was carried out on a Du Pont derivatograph model 1090B. Variable-temperature magnetic susceptibility (1.5–300 K) was carried out with a vibrating sample magnetometer. Diamagnetic corrections were made with Pascal's constants for all the constituent atoms.

Table 2. Atomic coordinates (×10^4) and equivalent isotropic thermal parameters (×10^3) for $[Fe_4O_2(O_2CC_2H_5)_7(bipy)_2]PF_6{\cdot}2H_2O$.

Atom	*x*	*y*	*z*	U_{eq}(Å^2)
Fe(1)	846(1)	2088(1)	4458(1)	44(1)
Fe(2)	473(1)	2916(1)	2386(1)	44(1)
O(1)	366(1)	2803(2)	3391(2)	43(1)
N(1)	1472(2)	1406(3)	5809(3)	58(1)
N(2)	1013(2)	3249(3)	5459(3)	54(1)
C(11)	1700(2)	476(4)	5908(4)	75(2)
C(12)	2140(3)	121(6)	6792(5)	99(2)
C(13)	2351(3)	763(7)	7545(5)	105(2)
C(14)	2120(3)	1693(7)	7434(4)	96(2)
C(15)	1670(2)	2021(4)	6553(3)	63(1)
C(16)	1387(2)	3020(4)	6371(3)	60(1)
C(17)	1488(3)	3712(7)	7061(4)	90(2)
C(18)	1215(3)	4621(7)	6820(5)	97(2)
C(19)	840(3)	4870(5)	5893(5)	88(2)
C(20)	750(2)	4166(4)	5234(4)	67(1)
O(21)	676(2)	1368(3)	2521(2)	60(1)
O(22)	867(2)	791(2)	3874(2)	63(1)
C(21)	792(2)	677(4)	3092(4)	57(1)
C(22)	847(4)	–408(5)	2840(6)	100(2)
C(23)	688(6)	–597(7)	1955(8)	145(4)
O(31)	478(1)	2815(3)	1228(2)	60(1)
O(32)	–208(1)	1646(3)	366(2)	62(1)
C(31)	266(2)	2069(4)	653(4)	61(1)

Table 2 (continuation)

C(32)	605(3)	1683(8)	275(6)	108(2)
C(33)	1158(6)	2222(9)	632(13)	187(6)
O(41)	326(2)	4472(3)	2316(2)	62(1)
C(41)	0	4905(6)	2500	71(2)
C(42)	0	6061(8)	2500	147(6)
C(43)	59(11)	6600(2)	3308(14)	163
O(51)	1570(1)	2677(3)	4571(2)	55(1)
O(52)	1309(1)	3302(3)	3184(2)	60(1)
C(51)	1651(2)	3238(4)	4064(3)	51(1)
C(52)	2191(2)	3855(5)	4496(4)	81(2)
C(53)	2467(4)	4110(8)	5530(6)	128(3)
P(1)	2500	2500	10000	100(2)
F(1)	2554(6)	3222(9)	9452(9)	160
F(2)	2791(6)	1819(10)	9745(10)	160
F(3)	1983(5)	2111(9)	9210(8)	160

RESULTS AND DISCUSSION

IR spectrum and TG analysis: At the range of 3000 ~ 3700 cm^{-1} of the IR spectrum, it is observed a strong broad band, which is ascribed to the vibration stretching of O–H bond of crystalline H_2O molecules. The spectrum bands at 1584, 1542, 1417, 1359 cm^{-1} show the strong peaks, which is due to the COO^- of coordinated propionate ions, while the characteristic absorption bands belong to the C–O and C=O disappears. The vibration frequencies from 1620 to 1590 cm^{-1} belonging to the phenyl ring of bipy do not appear and out-of-plane bending vibrations of hydrogen atom on the phenyl ring of bipy at the range of 720 ~ 920 cm^{-1} decrease to low frequency region, which indicates that the bipy participates in the coordination with Fe atoms.

The TGA of the complex shows a weight loss of 29.2% in the temperature range 344 ~ 398 K, corresponding to two molecules of water. The mass loss of 25.2% in the temperature range 399 ~ 456 K corresponds to the two bipy atoms. A successive mass loss of 41.5% was observed upon further heating, which is due to the loss of the propionate group.

Crystal structure: An ORTEP model of the title complex is shown in Fig. 1. Fig. 2 shows the coordination geometry for the Fe(III) atom. The selected bond distances and angles with the estimated standard deviations are listed in Table 3.

The crystal structure consists of a tetranuclear Fe(III) cation fragment and a PF_6^- anion. Among the four Fe(III) ions can be divided into two types according to the coordination environment around Fe atoms. One is six coordinated Fe(1) and Fe(1a) (Fig. 2 (a)), which both have two N atoms coordinated from the bipy ligand and four O atoms from the coordinated propionic acid group; another is the two “hinge” or “body” six coordinated Fe atoms Fe(2) and Fe(2a) (Fig. 2 (b)), which both have six

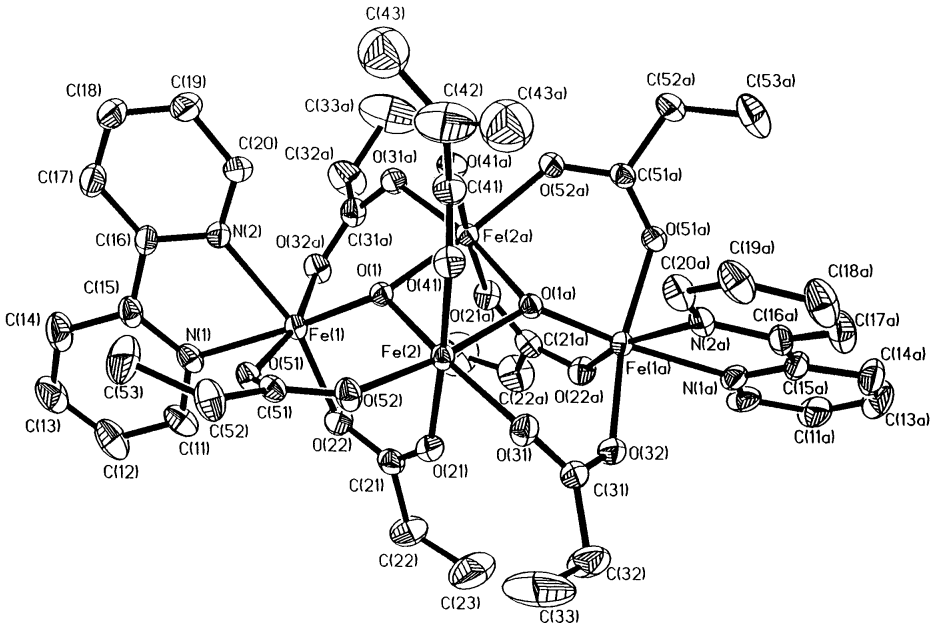

Figure 1. An ORTEP model of the compound $[Fe_4O_2(O_2CC_2H_5)_7(bipy)_2]PF_6 \cdot 2H_2O$ (hydrogen atoms were omitted for clarity).

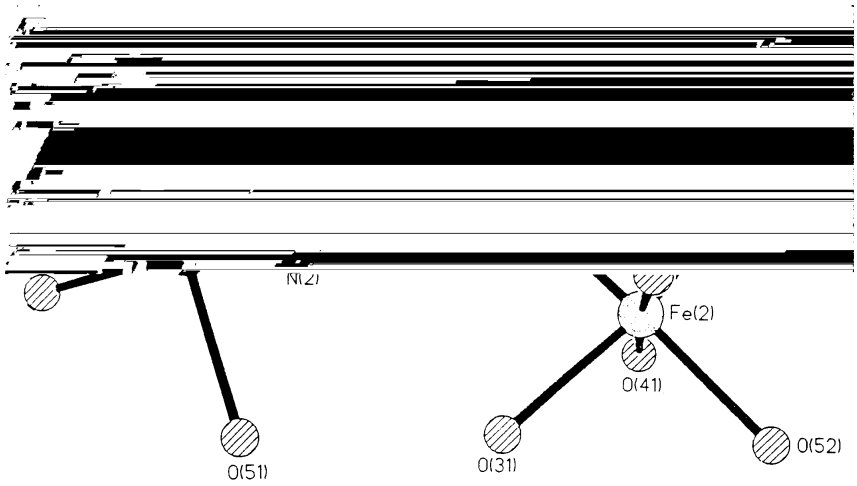

Figure 2. The coordination polyhedron for the four Fe atoms: (a) Fe(1) (Fe(1a)); (b) Fe(2) (Fe(2a)).

oxygen atoms from propionic acid ligand. The cation possesses a $Fe_4(\mu_3\text{-}O)_2$ bridging a "wing". The core can be considered as two edge-sharing Fe_3O triangular units with the oxygen atoms slightly below the Fe_3 planes. Peripheral ligation is provided by seven bridging $^{-}O_2CC_2H_5$ and two terminal chelating bipy groups, resulting in a distorted octahedral geometry about each Fe(III) sites. The two "hinge" or "body" Fe atoms (Fe(2) and Fe(2a)) are bridged by two oxides, whereas the wing-tip ions (Fe(1)

Table 3. Selected bond lengths (Å) and angles (°) for $[Fe_4O_2(O_2CC_2H_5)_7(bipy)_2]PF_6{\cdot}2H_2O$.

Fe(1)–O(1)	1.823(3)	Fe(2)–O(52)	2.006(3)
Fe(1)–O(32)a	2.047(3)	Fe(2)–O(31)	2.012(3)
Fe(1)–O(51)	2.064(3)	O(1)–Fe(2)a	1.953(3)
Fe(1)–N(2)	2.149(4)	Fe(2)–O(1)a	1.953(3)
Fe(1)–N(1)	2.185(4)	Fe(2)–O(41)	2.064(3)
O(32)–Fe(1)a	2.047(3)	Fe(2)–O(1)	1.924(3)
Fe(1)–O(22)	1.988(3)	Fe(2)–O(21)	2.077(4)
Fe(2)–Fe(2)a	2.8744(12)		
O(1)–Fe(1)–O(22)	97.76(13)	O(1)–Fe(1)–O(32)a	94.69(13)
O(22)–Fe(1)–O(32)a	96.08(15)	O(1)–Fe(1)–O(51)	92.14(12)
O(22)–Fe(1)–O(51)	93.74(15)	O(32)a–Fe(1)–O(51)	167.17(14)
O(1)–Fe(1)–N(2)	99.34(14)	O(22)–Fe(1)–N(2)	162.82(15)
O(32)a–Fe(1)–N(2)	84.11(15)	O(51)–Fe(1)–N(2)	84.07(14)
O(1)–Fe(1)–N(1)	173.20(15)	O(22)–Fe(1)–N(1)	87.94(15)
O(32)a–Fe(1)–N(1)	88.35(14)	O(51)–Fe(1)–N(1)	83.75(13)
N(2)–Fe(1)–N(1)	74.89(16)	O(1)–Fe(2)–O(1)a	83.63(12)
O(1)–Fe(2)–O(52)	95.77(12)	O(1)a–Fe(2)–O(52)	169.69(14)
O(1)–Fe(2)–O(31)	169.15(13)	O(1)a–Fe(2)–O(31)	88.63(12)
O(52)–Fe(2)–O(31)	93.20(13)	O(1)–Fe(2)–O(41)	90.20(13)
O(1)a–Fe(2)–O(41)	84.89(13)	O(52)–Fe(2)–O(41)	84.82(15)
O(31)–Fe(2)–O(41)	96.70(14)	O(1)–Fe(2)–O(21)	89.57(12)
O(1)a–Fe(2)–O(21)	98.70(13)	O(52)–Fe(2)–O(21)	91.58(15)
O(31)–Fe(2)–O(21)	84.06(14)	O(41)–Fe(2)–O(21)	176.36(14)
O(1)–Fe(2)–Fe(2)a	42.55(8)	O(1)a–Fe(2)–Fe(2)a	41.75(8)
O(52)–Fe(2)–Fe(2)a	135.23(10)	O(31)–Fe(2)–Fe(2)a	130.38(10)
O(41)–Fe(2)–Fe(2)a	80.82(10)	O(21)–Fe(2)–Fe(2)a	101.42(10)
Fe(1)–O(1)–Fe(2)	123.83(15)	Fe(1)–O(1)–Fe(2)a	131.54(15)
Fe(2)–O(1)–Fe(2)a	95.70(12)	C(11)–N(1)–Fe(1)	123.3(4)
C(15)–N(1)–Fe(1)	116.0(3)	C(20)–N(2)–C(16)	118.6(4)
C(20)–N(2)–Fe(1)	123.8(3)	C(16)–N(2)–Fe(1)	117.6(3)
C(21)–O(21)–Fe(2)	137.1(3)	C(21)–O(22)–Fe(1)	127.8(3)
C(31)–O(31)–Fe(2)	124.5(3)	C(31)–O(32)–Fe(1)a	129.0(3)
C(41)–O(41)–Fe(2)	125.4(4)	O(41)a–C(41)–O(41)	126.3(7)
C(51)–O(51)–Fe(1)	134.1(3)	C(51)–O(52)–Fe(2)	128.4(3)

Symmetry transformations used to generate equivalent atoms: a –x, y, –z + 1/2.

and Fe(1a)) have only a single oxide bridge (in addition to the $^{-}O_2CC_2H_5$). Consequently, the central Fe(2)–Fe(2a) separation is short, 2.8744(12) Å. The μ_3-O atoms bridge somewhat asymmetrically, the Fe(1)–O bond lengths range from 1.983(3) to 2.064(3) Å and the bond lengths of Fe(2)–O are in the range of 1.924(3) ~ 2.077(4) Å. It is noteworthy that the bong length of bridged O atom O(1) with Fe is the smallest. There exist seven propionate oxygen bridges to link up the four Fe atoms. The two nitrogen atoms are bonded to Fe atoms with a distance of 2.149(4) and 2.185(4) Å, respectively.

The bond angles of Fe–O(1)–Fe are: 123.83(15)° (Fe(1)–O(1)–Fe(2)), 131.54(15)° (Fe(1)–O(1)–Fe(2a)) and 95.70(12)° (Fe(2)–O(1)–Fe(2a)), respectively. The bond angles of the two μ O atoms with the Fe(2)–Fe(2a) bond are: 42.55(8)° (O(1)–Fe(2)–Fe(2a)) and 41.75(8)° (O(1a)–Fe(2)–Fe(2a)), respectively. The bond angles of other four O atoms with Fe(2)–Fe(2a) bond are ranged from 80.82(10)° to 135.23(10)°. The four Fe atoms belong to tetrahedron conformation and form the four tetrahedron framework in the complex system, so the complex has the bent "butterfly" structure similar to the report [10–12]. Gorun and Lippard have carried out detailed analyses of the core geometry in butterfly structural types [11]. The whole complex molecule is a symmetry structure and the symmetrical axis is linking line of Fe(2) and Fe(2a). The six propionate groups provide the twelve oxygen atoms to bridge the different types of Fe atoms, that is to say, Fe(1) and Fe(2), Fe(1a) and Fe(2a). It is different that the seventh propionate group links up the same types of Fe atoms Fe(2) and Fe(2a), which provides the two oxygen atoms O(41) and O(41a). Fig. 3 shows the packing unit cell diagram for the title complex.

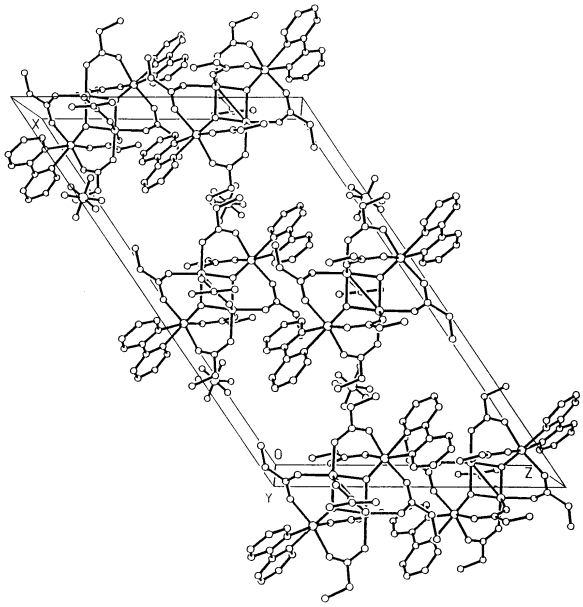

Figure 3. Packing diagram of unit cell of $[Fe_4O_2(O_2CC_2H_5)_7(bipy)_2]PF_6{\cdot}2H_2O$.

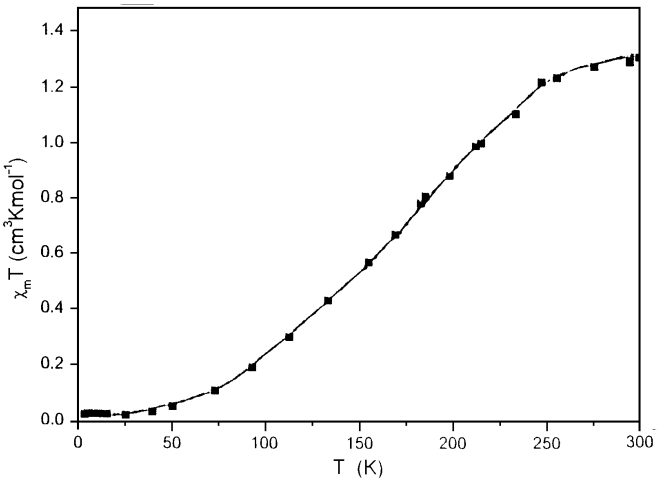

Figure 4. Temperature dependence of magnetic susceptibility for the title complex, experimental (■) and calculated (—).

Magnetic properties: The magnetic susceptibility of title complex was measured at 10000 Oe in the range from 3 ~ 300 K (Fig. 4). A plot of molar magnetic susceptibility $\chi_m T$ versus temperature is given in Fig. 4. The $\chi_m T$ gradually decreases from 1.334 cm^3Kmol^{-1} at 300 K and tends to 0.022 cm^3Kmol^{-1} at 3.0 K, which indicates an overall antiferromagnetic behavior. The data clearly indicate that the title complex possesses an $S = 0$ ground state, in accord with what has been observed in [11,12]. In a qualitative sense, the $S = 0$ state can be thought of in terms of an antiferromagnetic coupling of the four high-spin Fe(III) ions to produce a ground state of zero net spin.

As indicated earlier [12], the basic $[Fe_4O_2]^{8+}$ core structure of the title complex is essentially described as the so-called "butterfly". The magnetic exchange interactions in this system can be described in a similar fashion by use of the isotropic spin Hamiltonian given in the following equation:

$$H = -2J_{wb}(S_1 \cdot S_2 + S_2 \cdot S_{1'} + S_{1'} \cdot S_{2'} + S_2 \cdot S_1) - 2J_{bb}(S_2 \cdot S_{2'})$$

In this equation J_{wb} describes the "wing-body" exchange interactions about the periphery of the tetranuclear core, and J_{bb} describes the "body-body" or "hinge" interaction of the two central Fe(III) ions. Then numbering scheme for the $S_i \cdot S_j$ terms is that used in Fig. 1. Defining $S_A = S_1 + S_{1'}$, $S_B = S_2 + S_{2'}$, and $S_T = S_A + S_B$, equivalent-operator replacements can be made for all $S_i \cdot S_j$ terms in the above equation. The resulting eigenvalue equation was then used in the van Vleck equation to derive an expression for the molar paramagnetic susceptibility of the complex.

$$E = -J_{wb}[S_T(S_T + 1) - S_A(S_A + 1) - S_B(S_B + 1)] - J_{bb}[S_B(S_B + 1)]$$

The detailed discussion can be find in [12]. Least squares fitting leads to $J_{wb} = -41.6$ cm^{-1}, $J_{bb} = -7.3$ cm^{-1}, $g = 2.02$, and $R = 6.8 \times 10^{-4}$, respectively, where R is the agree-

ment factor defined as $R = \{\Sigma[(\chi_m T)_{obs}(i)-(\chi_m T)_{calcd}(i)]^2/\Sigma\,[(\chi_m T)_{obs}(i)]^2\}$. The negative values of J_{wb} and J_{bb} also reveal an antiferromagnetic between Fe^{III} ions in the complex. From Fig. 4, it is clear that the theoretical curve fits the experimental data quite well.

In conclusion, a novel tetranuclear Fe(III) complex $[Fe_4O_2(O_2CC_2H_5)_7(bipy)_2]PF_6\cdot 2H_2O$ has been prepared and the structural analysis shows that the complex has an interesting "butterfly" core structure $[Fe_4O_2]^{8+}$, which is a new example of tetranuclear Fe(III) complex belonging to "butterfly" core structure similar to the reports [10,12]. The crystal structure data of the title complex is similar to that of tetranuclear Fe(III) complex using acetic acid bridge, but different from the tetranuclear Fe(III) complex using benzoic acid bridge. This is due to the larger steric hindrance of the larger phenyl cycle group in the later ligand. The corresponding variable temperature susceptibility measurement shows the antiferromagnetic interactions in the complex, which is similar to that of other known tetranuclear complexes with "butterfly " core structure.

Acknowledgments

This work was supported by the National Natural Science Foundation of China (29831010, 20023005), the State Key Project of Fundamental Research of China (G1998061306) and the China Postdoctoral Science Foundation.

REFERENCES

1. Lippard S.J., *Angew. Chem. Int. Ed. Engl*., **27**, 344 (1988).
2. Donald M.K., *Chem. Rev.*, **90**, 585 (1990).
3. Konno M. and Kido M.M., *Bull. Chem. Soc. Jpn*., **64**, 33 (1991).
4. Wilkins P.C. and Wilkins R.G., *Coord. Chem. Rev.*, **79**, 195 (1987).
5. Sheriff S., Hendrichkson W.A. and Smith J.L., *J. Mol. Bio*l., **197**, 273 (1987).
6. Fox B.G., Surerus K.K., Munck E. and Lipscomb J.D., *J. Biol. Chem*., **263**, 10553 (1988).
7. Ericson A., Hedman B., Hodgson K.O., Green J., Dalton H., Bentsen J.G., Gbeer R.H. and Lippard S.J., *J. Am. Chem. Soc*., **110**, 2330 (1988).
8. Nordlund P., Sjoberg B.M. and Eklund H., *Nature*, **345**, 593 (1990).
9. Averill B.A., Davis J.C., Bruma S., Zirino T., Sanderts-Loehr J., Loehr T.M., Sage J.T. and Debrunner P.G., *J. Am. Chem. Soc*., **109**, 3670 (1987).
10. Armstrong W.H., Roth M.E. and Lippard S.J., *J. Am. Chem. Soc*., **109**, 6318 (1987).
11. Gorun S.M. and Lippard S.J., *Inorg. Chem*., **27**, 149 (1988).
12. McCusker I.M., Vincent I.B., Schmitt E.A., Mino M.L., Shin K., Coggin D.K., Hagen P.M., Huffman I.C., Christou G. and Hendrickson D.N., *J. Am. Chem. Soc*., **113**, 3012 (1991).